Innovare Academic Sciences

International Journal of Pharmacy and Pharmaceutical Sciences

ISSN- 0975-1491 Vol 6, Issue 4, 2014

Original Article

FORMULATION AND CHARACTERIZATION OF RIFAMPICIN-LOADED P(3HB-*co*-4HB) NANOPARTICLES

***AMIRAH M.G.[1,2], AMIRUL A.A[2,3], HABIBAH A. WAHAB[1,2]**

[1]School of Pharmaceutical Sciences, Universiti Sains Malaysia, 11800 Penang, Malaysia.[2]Malaysian Institute of Pharmaceutical and Nutraceutical (IPharm), Ministry of Science, Technology and Innovation (MOSTI), Halaman Bukit Gambir, 11700 Penang, Malaysia.[3]School of Biological Sciences, Universiti Sains Malaysia, 11800 Penang, Malaysia.

Email: amirahmohdgazzali@gmail.com.

Received: 05 Jan 2014 Revised and Accepted: 23 Jan 2014

ABSTRACT

Objective: Many studies carried out on nanoparticles for drug delivery employed Poly (lactide-*co*-glycolide) copolymer as the encapsulating polymer. In this study, we used a locally produced copolymer, Poly (3-hydroxybutyrate-*co*-4-hydroxybutyrate) to encapsulate rifampicin, a hydrophobic drug. This paper aims to describe the characteristics of the nanoparticles formed and its drug release capability.

Methods: Two types of nanoparticles were prepared; rifampicin-loaded nanoparticles and chitosan-coated rifampicin-loaded nanoparticles through emulsification/solvent evaporation method. The properties of these nanoparticles were evaluated and compared.

Results: Preliminary study showed that both the uncoated nanoparticles and the chitosan-coated nanoparticles produced particles with average sizes < 200 nm with polydispersity index, PDI < 0.200 and < 250 nm with PDI < 0.400, respectively. The uncoated nanoparticles had the highest encapsulation of 26.58% whilst the chitosan-coated nanoparticles encapsulated 14.43% rifampicin. Both types of particles are fairly spherical. *In vitro* release studies showed that the encapsulated rifampicin in uncoated nanoparticles was completely released in 10 hours regardless of the medium pH whereas only 81.30% was released in 10 hours at pH 4.5 from the chitosan-coated nanoparticles.

Conclusion: The findings of this study suggested that the production of nanoparticles with good physical characteristics is possible from this novel copolymer and the copolymer has a huge potential to be used further in formulation development of nanoparticles.

Keywords: P (3HB-*co*-4HB), Nanoparticles, Rifampicin, Chitosan

INTRODUCTION

The application of nanoparticles in drug delivery of pharmaceuticals offers many advantages to the overall treatment strategies and therapy outcomes. Nanoparticles are very versatile and its design could be tailored to the needs of individual drug. Simple biodegradable polymeric nanoparticles as an example, are able to provide controlled release of the encapsulated drug and hence the therapeutic efficacy of the drug could be prolonged and enhanced with subsequent reduction in its side effects [1].

Among the many types of polymer available, PLGA is the most commonly used copolymer in drug delivery researches. In this study however, we used Poly (3-hydroxybutyrate-*co*-4-hydroxybutyrate) or P (3HB-*co*-4HB), a copolymer produced from cultivation of a novel bacterium species, *Cupriavidus sp*. USMAA1020 [2].

The monomers could naturally be found as metabolites in human body and hence the copolymer is believed to be biocompatible with the human body system [3-5].

Previous studies had successfully produced microparticles from other types of polyhydroxybutyrate polymer [5,6], but to our knowledge, no study on the production of nanoparticles from P (3HB-*co*-4HB) has been reported.

The emergence of PHB-group of polymers as potential cheap biomaterial may also become an interesting alternative in the production of controlled release matrix.

This study investigated the potential of producing nanoparticles from P (3HB-*co*-4HB) copolymer. In addition to this type of nanoparticles, a type of coated nanoparticles was also produced by using chitosan as the coating material. Rifampicin, an anti-tuberculosis drug was chosen to be incorporated in both type of nanoparticles produced. The nanoparticles characteristics were then evaluated and our findings were reported in this publication.

MATERIALS AND METHODS

Materials

The copolymer of P (3HB-*co*-4HB) with 68% - 70% 4HB content was a gift from Bio-Process Division, Malaysian Institute of Pharmaceutical and Nutraceutical (IPharm, MOSTI). The stabilizer used was Poly (vinyl alcohol), PVA with molecular weight of 9,000 to 10,000 g/mol and 80% hydrolysed (Sigma, USA). Rifampicin was supplied by BioBasic, Canada (purity ≥ 97%). Chitosan was from Acros®, with molecular weight of 100,000 to 300,000. The oil phase used to solubilise the copolymer was dichloromethane, analytical reagent grade (QReC™). Trehalose dihydrate was obtained from Calbio-Chem® and potassium bromide for infra-red spectroscopy was from Fisher Scientific. The phosphate buffered saline tablet (pH 7.4) was from Calbio-Chem®, whilst acetic acid glacial was from Systerm® ChemAR and sodium acetate trihydrate was obtained from J&J®. The L-ascorbic acid was from Calbio-Chem®. Ultrapure water was used throughout the study and was purified by Milli-Q® Biocel water purification system (Millipore, France).

Methods

Pre-formulation study of P (3HB-*co*-4HB) nanoparticles

The pre-formulation study was conducted by varying one parameter at a time and controlling the others as to see the effect of certain parameters on the average particles size produced. The best combination of processing parameters was then chosen to produce rifampicin-loaded nanoparticles.

Briefly, P (3HB-*co*-4HB) copolymer was weighed carefully and dissolved in dichloromethane (DCM) at a ratio of 10:1. In a separate bottle, PVA was dissolved in deionised water. The DCM solution was then poured into the solution of stabilizer and immediately homogenized for 5 minutes by IKA® T25 Digital Ultra-Turrax® before being subjected to sonication (Sartorius Labsonic® M probe

sonicator). Next, the resultant oil-in-water emulsion was transferred onto a magnetic stirring plate and continuously stirred overnight at room temperature, 550 rpm to completely remove the DCM via evaporation.

In the case of fast solvent evaporation method, the solvent evaporation was carried out by using a rotary evaporator (IKA® RV 10 control) set at 300 mbar and 100 rpm at ambient temperature until the bubble formation ceased.

After the solvent evaporation process was completed, the average particles size and polydispersity index of nanoparticles were determined by using Malvern Zetasizer Nano ZS (Malvern Instrument, Malvern, UK). In the case of chitosan-coated nanoparticles, the chitosan was dissolved together with PVA in acetate buffer pH 4.4.

Formulation of rifampicin-loaded P (3HB-*co*-4HB) nanoparticles

Based on the results from the pre formulation study, Subsection 2.2, different formulations of rifampicin-loaded nanoparticles were produced and were then subjected to evaluation on their encapsulation efficiencies, drug loading capacity and percentage of yield. The nanoparticles were prepared as outlined in Table 1 and 2. After completion of solvent evaporation process, the nanoparticles suspension was centrifuged at 5,000 rpm for 10 minutes and the recovered supernatant was further centrifuged at 21,000 rpm for 2 hours. The pellet produced after this centrifugation was re-dispersed in trehalose dihydrate solution and subsequently freeze-dried. The particles suspension was freeze at -80ºC for 12 hours and dried by freeze-dryer Labconco® FreeZone[6] for 48 hours. The free-flowing nanoparticles powders were then kept in desiccators until further analysis.

Table 1: The five formulations of rifampicin-loaded P (3HB-*co*-4HB) nanoparticles prepared.

Formulation	Fabrication method	PVA concentration	Rifampicin amount (mg)	Rate of Solvent evaporation
F1	Homogenization (23,000 rpm, 5minutes) and Sonication (10 minutes)	3%	100	Fast
F2	Homogenization (23,000 rpm, 5minutes) and Sonication (10 minutes)	3%	100	Slow
F3	Homogenization (23,000 rpm, 5 minutes)	3%	100	Fast
F4	Homogenization (23,000 rpm, 5minutes) and Sonication (10 minutes)	2%	100	Fast
F5	Homogenization (23,000 rpm, 5minutes) and Sonication (10 minutes)	3%	50	Fast

Table 2: The five formulations of chitosan-coated rifampicin-loaded P (3HB-*co*-4HB) nanoparticles prepared.

Formula	Fabrication method	PVA concentration	Chitosan concentration	Rifampicin (mg)	Solvent evaporation
CF-1	Homogenization (23,000 rpm, 5minutes) and Sonication (10 minutes)	3%	0.5%	50	Fast
CF-2	Homogenization (23,000 rpm, 5minutes) and Sonication (10 minutes)	3%	0.5%	50	Slow
CF-3	Homogenization (23,000 rpm, 5minutes) and Sonication (10 minutes)	3%	1.0%	50	Fast
CF-4	Homogenization (23,000 rpm, 5minutes) and Sonication (10 minutes)	2%	0.5%	50	Fast
CF-5	Homogenization (23,000 rpm, 5minutes) and sonication (5 minutes)	3%	0.5%	50	Fast

The amount of rifampicin encapsulated was determined by analyzing the content of drug available in the nanoparticles powder. A known amount of freeze-dried nanoparticles was dissolved in 1 ml of dichloromethane and an excessive amount of methanol, 9 ml was added. The solution was then centrifuged by ultrafiltration at 10,000 rpm and the filtrate was further diluted with phosphate-buffered saline. The amount of rifampicin available was then determined by UV/VIS Spectrophotometer at 475 nm [7]. The encapsulation efficiency, EE% of rifampicin in the formulation was calculated as the percentage of the amount of rifampicin available in the formulation against that of the amount of rifampicin initially incorporated in the formulation:

$$EE\% = \frac{\text{Amount of rifampicin available in the formulation (mg)}}{\text{Amount of rifampicin incorporated in the formulation (mg)}} \times 100$$

The percentage of drug content was determined by calculating the amount of drug available in the formulation against the amount of nanoparticles recovered [8]:

$$\text{Drug content } (\%\tfrac{w}{w}) = \frac{\text{Amount of rifampicin available in the formulation (mg)}}{\text{Amount of nanoparticles recovered (mg)}} \times 100$$

Yield of nanoparticles was calculated based on the weight of nanoparticles powder recovered after completion of the whole formulation process [9]:

$$\text{Yield } \% = \frac{\text{Weight of nanoparticles recovered (mg)}}{\text{Initial amount of co polymer and drug used (mg)}} \times 100$$

Transmission electron microscopy

The morphology of the nanoparticles was analyzed by Transmission Electron Microscope (CM12® FEI, Eindhoven, the Netherlands). Diluted samples were dropped on a sample grid and visualize under the microscope.

Fourier-transform infra-red (FTIR) analysis

Two different analysis techniques were used; the potassium bromide (KBr) method and attenuated total reflectance (ATR) method. Pure rifampicin powder was analyzed by the KBr method, whilst the crude copolymer, chitosan-coated unloaded nanoparticles and chitosan-coated rifampicin-loaded nanoparticles were subjected to the ATR method. In the KBr method, approximately 1 mg of

sample were ground with 100 mg of potassium bromide (KBr) and compressed with compaction force of 16 tons cm^{-2} and holding for 1 minute by using IR hydraulic press pump (Backman PIG, UK). In the ATR method, samples were directly placed on a crystal surface and clamped. For both methods, the equipment (Nicolet, Impact 410, USA) was set to take sixteen scans of each sample in the region 400 to 5,000 cm^{-1}. The spectra produced were then analyzed by using Omnic software (Thermo Nicolet, USA).

Effect of aging on nanoparticles size and polydispersity index

The nanoparticles powders were kept at three different temperatures: 4ºC, 25ºC and 40ºC in containers filled with silica beads for 90 days. Every 14 days, the nanoparticles were evaluated for its average particles size and polydispersity index.

***In vitro* drug release study and kinetics of release**

The *in vitro* drug release study of the encapsulated rifampicin was conducted in three different buffers; acetate buffer pH 4.5, phosphate buffer pH 6.8 and phosphate buffer pH 7.4, each containing ascorbic acid. Briefly, an amount of freeze-dried nanoparticles equivalent to 1 mg of rifampicin was dispersed in 2 ml of buffer and transferred into dialysis tube (MWCO : 12,000 – 14,000). The tube was then immersed in 50 ml of medium and incubated in an incubator shaker set at 37.5ºC and rotated horizontally at 100 rpm. At specific time intervals, the dialysis tube was taken out and immediately transferred into a new medium pre-warmed at the same temperature to continue the release study. The used medium was analyzed for the content of rifampicin release by UV/VIS Spectrophotometer at 475 nm. The data obtained was then fitted into different release kinetics models; zero order, first order, Hixson-Crowell release model, Higuchi release model and Korsmeyer-Peppas release model.

Statistical Analysis

T-test and Analysis of Variance (ANOVA) was performed by means of SPSS software to compare between results. P values of less than 0.05 were accepted as statistically significant results.

RESULTS & DISCUSSION

Pre-formulation study of P (3HB-*co*-4HB) nanoparticles

The pre-formulation study of P (3HB-*co*-4HB) nanoparticles revealed the influence of several processing parameters on the average nanoparticles size. Particles size was significantly increased from 239.2 nm to 390.6 nm with the increment in PVA concentration from 1% to 5% (*P < 0.05), which was due to the presence of more PVA molecules on the surface of the nanoparticles.

The application of homogenization force at 23,000 rpm on the nanoparticles emulsion was shown to reduce the average particles size significantly as compared to applying only 13,000 rpm homogenization strength (425.8 nm and 1989.0 nm respectively). Sonication which is another type of particles reduction method was also tested as an alternative to homogenization. It shows similar trend in which the average particles size was significantly reduced from 273.6 nm to 231.0 nm by increasing the sonication time from 5 minutes to 10 minutes (*P < 0.05).The combination of homogenization and sonication on the other hand produced particles with better uniformity as compared to either homogenization or sonication alone. This part of study was conducted by maintaining the homogenization at a constant rate and time; 23,000 rpm and 5 minutes, and varying the sonication time. It was found that with the increment in sonication time, the average particles size was reduced significantly from 257.8 nm to 216.0 nm, from 5 minutes to 15 minutes (*P < 0.05). Combining both methods also produced particles with better uniformity, with polydispersity index of less than 0.200. Rate of solvent evaporation was found to have no significant effect on the average nanoparticles size. Fast solvent evaporation method produced particles of 253.6 nm whilst slow solvent evaporation method produced particles with size of 267.4 nm. The average particles size of chitosan-coated nanoparticles was shown to be increased concurrently with the increment in chitosan concentration. By increasing the concentration from 0.1% to 0.25%, the average particles size was increased from 155.4 nm to 193.5 nm. This increment in the particles size is most probably due to the presence of more chitosan molecules on the particles surface with the addition of higher chitosan concentration in the formulation. Zeta potentials of the nanoparticles were also increased from +11.6 mV to +19.9 mV with increment in chitosan concentration, indicating that more chitosan molecules were firmly adsorbed and immobilized on the particles' surface which causes the suppression of the original negative charge imparted by the uncoated nanoparticles (data not shown). Increasing the copolymer concentration in the formulation was also shown to increase the nanoparticles size. By increasing the copolymer concentration from 0.125% to 0.5%, the average nanoparticle sizes increased from 156.0 nm to 181.0 nm.

Formulation of rifampicin-loaded P (3HB-*co*-4HB) nanoparticles

Table 3 and Table 4 showed the different nanoparticles prepared and their encapsulation efficiencies, percentage of drug content and percentage of yield. In the case of uncoated nanoparticles, the percentage of rifampicin encapsulation was between 11.05% w/w and 26.58% w/w. The highest encapsulation efficiency (EE%) was from formulation F4 which was prepared by reducing the concentration of PVA used in the formulation. The lowest EE% on the other hand was given by formulation F3 which was prepared by homogenization alone method, without sonication. This showed that sonication might have a beneficial effect on increasing EE% of rifampicin within the nanoparticles. Slow solvent evaporation process (F2) produced higher EE% than the formulation prepared by fast solvent evaporation (F1); 21.37% w/w as compared to 16.89% w/w. Percentage of drug content varied between the different formulations. Formulation F4 recorded the highest percentage with 27.30% w/w of rifampicin present in the nanoparticles. Percentage of yield obtained was varied between 33.33% and 68.83% w/w. Yield of nanoparticles from formulation F1 and F2 did not differ significantly; showing that rate of solvent evaporation has no influence on nanoparticles yield (Table 3).

Table 3: The effect of different processing parameters on EE%, rifampicin content and yield of rifampicin-loaded nanoparticles

Formula	SE[1]	HG[2]	RIF[5] (mg)	[PVA] (%)	EE (%)	RIF[5] content (%)	Yield (%)
F1	Fast	H/S[3]	100	3	16.89±0.02	12.53±0.02	67.83±0.04
F2	Slow	H/S[3]	100	3	21.37±0.01	15.55±0.01	68.83±0.04
F3	Fast	H[4]	100	3	11.05±0.03	16.30±0.03	33.33±0.03
F4	Fast	H/S[3]	100	2	26.58±0.04	27.30±0.05	49.33±0.04
F5	Fast	H/S[3]	50	3	20.61±0.03	8.59±0.02	-

* Values are expressed as mean ± SD (n=3),[1]Solvent evaporation rate,[2] Homogenization methods,[3] Homogenization and sonication,[4] Homogenization alone.[5] Rifampicin.

The chitosan-coated, rifampicin-loaded nanoparticles gave lower percentages of encapsulated rifampicin (Table 4) as compared to the uncoated rifampicin-loaded nanoparticles, in which the highest EE% obtained was only 14.43%. Formulation CF-2 which produced this highest EE% was prepared via slow solvent evaporation method. Slow solvent removal might give more time for the entrapment of rifampicin within the chitosan network as the formation of chitosan coating might be a slow process. Percentage of rifampicin content on

the other hand did not show any significant difference between the five formulations. In term of yield percentage, formulation CF-2 gave the highest yield, 82.83% and this showed that the slow solvent evaporation process is an efficient method for the production of chitosan-coated rifampicin-loaded nanoparticles.

Table 4: The effect of different processing parameters on EE%, rifampicin content and yield of chitosan-coated rifampicin-loaded nanoparticles

Formula	SE[1]	HG[2]	Chitosan (%)	[PVA] (%)	EE (%)	RIF[5] content (%)	Yield (%)
CF-1	Fast	H/S[3]	0.5	3	11.37±1.58	4.51±0.007	63.83±4.6
CF-2	Slow	H/S[3]	0.5	3	14.43±1.03	4.36±0.004	82.83±4.6
CF-3	Fast	H/S[3]	1.0	3	10.46±1.81	4.27±0.010	46.27±8.1
CF-4	Fast	H/S[3]	0.5	2	7.30±1.85	4.25±0.003	43.77±3.3
CF-5	Fast	H/S[4]	0.5	3	9.09±0.38	4.43±0.003	51.50±4.4

* Values are expressed as mean ± SD (n=3),[1] Solvent evaporation rate,[2] Homogenization methods,[3] Homogenization and sonication,[4] Homogenization and sonication (5 minutes),[5] Rifampicin

Transmission electron microscopy

The images obtained from TEM showed that the particles from both types of nanoparticles were fairly spherical. Their sizes as projected by TEM were similar to those obtained by dynamic light scattering (DLS) method. These images had hence confirmed the success of nanoparticles production by this method.

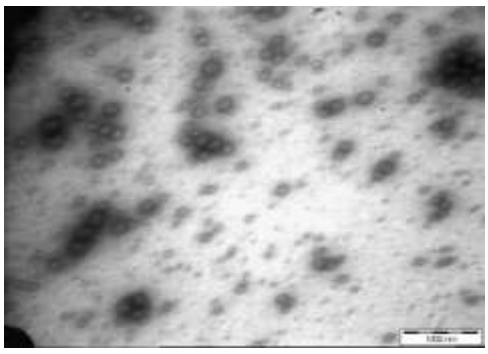

Fig. 1: TEM image of rifampicin-loaded P (3HB-*co*-4HB) nanoparticles.

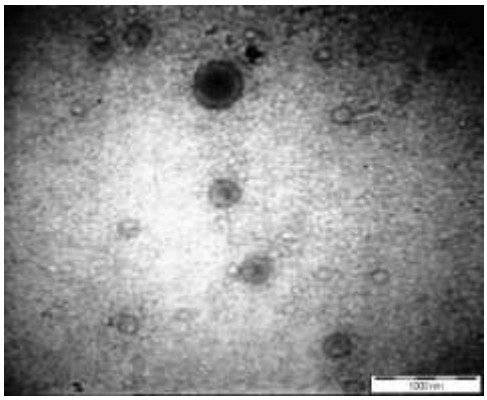

Fig. 2: TEM image of chitosan-coated P (3HB-*co*-4HB) nanoparticles. Note the presence of chitosan-coating layer around the nanoparticles.

Fourier-transform infra-red (FTIR) analysis

The FTIR spectrum of pure rifampicin showed several characteristic peaks; absorption band of O-H and N-H at 3432 cm^{-1}, the C-H stretching at 2938 cm^{-1}, -C=O acetyl stretching at 1732 cm^{-1}, -C=N asymmetric stretching at 1650 cm^{-1}, C=C stretching at 1569 cm^{-1}, C-N stretching at 1373 cm^{-1}, –C-O-C- ether group at 1254 cm^{-1} and C=C bending at 976 cm^{-1} (10)

The crude P (3HB-*co*-4HB) copolymer showed an intense absorption peak at 1720 cm^{-1} which represented the C=O functional group. A peak was also visible at 1172 cm^{-1} corresponding to the asymmetric stretching of the C-O-C group [11-13]. Formulated blank nanoparticles showed similar peaks. The 1720 cm^{-1} peak was prominently visible, whilst the 1291 cm^{-1} peak was slightly shifted to 1262 cm^{-1} and the 1172 cm^{-1} peak was shifted to 1176 cm^{-1}.

The rifampicin-loaded nanoparticles maintained some of the rifampicin peaks with slight shifting. Peaks corresponding to rifampicin at 2938 cm^{-1} and 1254 cm^{-1} are detectable. The main peaks associated with P (3HB-*co*-4HB) copolymer could also be seen in the rifampicin-loaded nanoparticles spectrum, such as the absorption peaks at 1724 cm^{-1} and 1172 cm^{-1}.

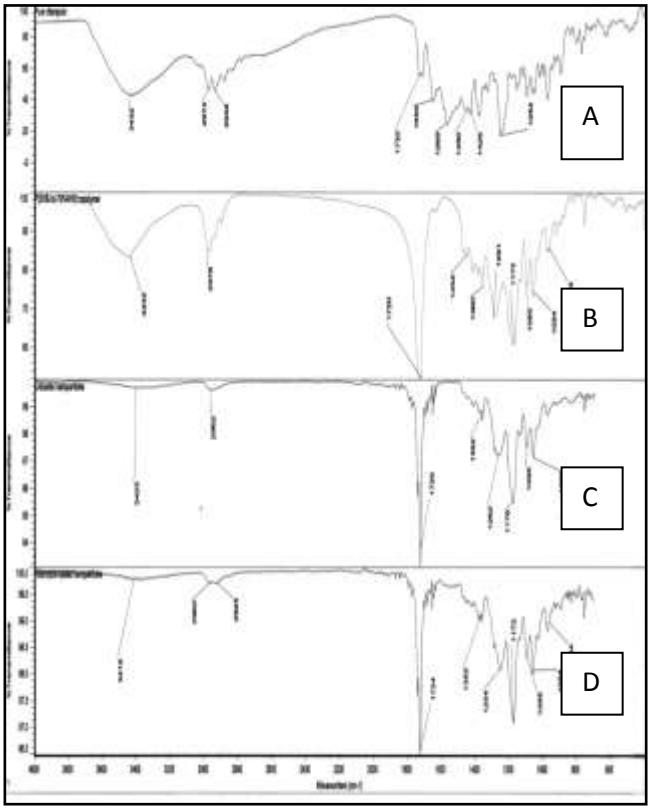

Fig. 3: The FTIR spectrums for uncoated P (3HB-*co*-4HB) nanoparticles. (A: Rifampicin. B: P (3HB-*co*-4HB) copolymer. C: Blank nanoparticles. D: Rifampicin-loaded nanoparticles.)

The FTIR spectrum of chitosan (Figure 4) showed a broad absorption band at 3444 cm^{-1} corresponding to the N-H and O-H stretching, 1646 cm^{-1} related to the N-H deformation peak from the glucosamine unit and 1078 cm^{-1} associated with the C-O-C stretching.

The 2921 cm^{-1} and 2880 cm^{-1} peaks were attributed to C-H stretching. The N-H deformation peak was the result of deacetylation, due to the deacetylated nature of the chitosan used in this study. Chitosan infra-red spectrum prior to deacetylation usually will show a primary amide peak at 1656 cm^{-1}. This primary amide band will diminish according to the degree of deacetylation and the 1646 cm^{-1} will then become more prominent [14].

Analysis on the unloaded chitosan-coated nanoparticles showed that several major peaks of chitosan were present with slight shifting. The 3444 cm^{-1} peak was shifted to 3350 cm^{-1} and the 2921 cm^{-1} peak was shifted to 2933 cm^{-1}. The 1720 cm^{-1} peak associated with P (3HB-*co*-4HB) copolymer was sharply visible but with slight shifting to 1724 cm^{-1}.

A peak was also visible at 1654 cm^{-1} indicative of the N-H deformation peak from the glucosamine units present in chitosan. The 1078 cm^{-1} peak on the other hand was shortened, suggesting the possibility of some interaction between chitosan and P (3HB-*co*-4HB) at the C-O-C position.

As for chitosan-coated rifampicin-loaded nanoparticles, the spectrum showed a broad peak at 3371 cm^{-1}. This was attributed to the presence of –OH and –NH groups in all components of the formulation; rifampicin, P (3HB-*co*-4HB) copolymer and chitosan which led to formation of a broad band in the spectrum. The presence of a prominent peak at 1413 cm^{-1} (C-H bending) could be contributed by the C-H that present in rifampicin, the copolymer and also chitosan.

Effect of aging on nanoparticles size and polydispersity index

The average size of particles kept at 4ºC and 25ºC were satisfactorily preserved over the period of evaluation (Table 5). These particles were also easily dispersed upon reconstitution with no apparent agglomeration. No changes in particles flowability was observed throughout the experimental period.

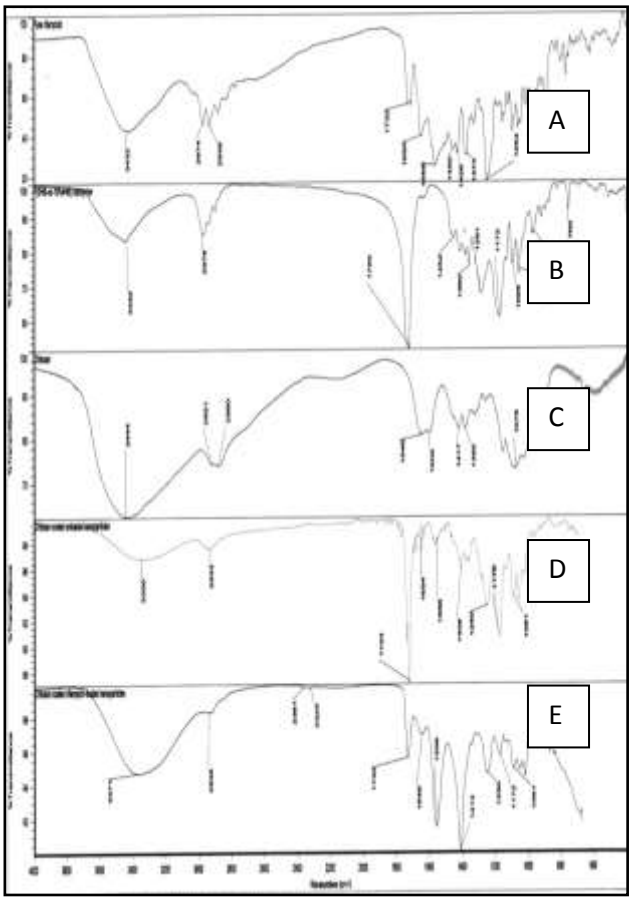

Fig. 4: The FTIR spectrums for chitosan-coated P (3HB-*co*-4HB) nanoparticles (A: Rifampicin. B: P (3HB-co-4HB) copolymer. C: Chitosan. D: Chitosan-coated blank nanoparticles. E: Chitosan-coated rifampicin-loaded nanoparticles.)

Table 5: The effect of aging on the average particles size of rifampicin-loaded P (3HB-*co*-4HB) nanoparticles

	Temperature (ºC)		
Week	4	25	40
0	189.7 ± 2.0	193.9 ± 0.4	185.2 ± 1.1
2	187.4 ± 1.8	195.2 ± 2.0	309.8 ± 4.1
4	186.0 ± 0.8	191.4 ± 1.5	303.1 ± 2.9
6	186.5 ± 2.7	181.2 ± 1.1	324.0 ± 0.4
8	184.2 ± 0.9	184.8 ± 1.2	340.2 ± 10.3
10	196.4 ± 0.9	195.1 ± 1.3	320.9 ± 4.3
12	186.6 ± 1.5	192.3 ± 0.8	332.1 ± 3.5

The average size of nanoparticles kept at 40ºC however, increased over the period of study. The particles were agglomerated which was evidence from the increment in particles size and the polydispersity index as detected by zetasizer. There was also reduction in the flowability of the nanoparticles powder with visual presence of aggregation.

Table 6: The effect of aging on the average particles size of chitosan-coated rifampicin-loaded P (3HB-*co*-4HB) nanoparticles

	Temperature (ºC)		
Week	4	25	40
0	220.2 ± 2.0	220.2 ± 2.0	220.2 ± 2.0
2	218.4 ± 2.0	280.8 ± 2.1	298.1 ± 5.8
4	258.9 ± 3.2	301.3 ± 8.0	314.0 ± 2.4
6	257.8 ± 1.5	318.1 ± 4.2	314.5 ± 2.2
8	249.1 ± 3.5	332.3 ± 1.9	323.5 ± 1.5
10	300.6 ± 4.4	378.5 ± 8.4	359.4 ± 9.5
12	299.4 ± 8.5	393.9 ± 8.5	364.6 ± 9.8

Table 7: The values of R^2 from release kinetic models fitting on the *in vitro* drug release data of rifampicin nanoparticles in acetate buffer pH 4.5, phosphate buffer pH 6.8 and phosphate buffer pH 7.4.

Buffer	Zero-order	First-order	Hixson-Crowell	Higuchi	Korsmeyer-Peppas
pH 4.5	0.9719	0.9853	0.9974	0.9988	1.000 (n = 0.5743)
pH 6.8	0.9563	0.9989	0.9869	0.9947	0.9996 (n = 0.5954)
pH 7.4	0.9855	0.9909	0.9985	0.9987	0.9996 (n = 0.5788)

Table 8: The values of R^2 from release kinetic models fitting on the *in vitro* drug release data of chitosan-coated rifampicin-loaded nanoparticles in acetate buffer pH 4.5, phosphate buffer pH 6.8 and phosphate buffer pH 7.4.

Buffer	Zero order	First order	Hixson-Crowell	Higuchi	Korsmeyer-Peppas
pH 4.5	0.9767	0.9979	0.9909	0.9997	0.9997 (n = 0.42790)
pH 6.8	0.9632	0.9952	0.9941	0.9966	1.000 (n = 0.5206)
pH 7.4	0.9898	0.9966	0.9930	0.9979	0.9999 (n = 0.5532)

At 4ºC and 25ºC, the presence of glassy network of trehalose as the cryoprotectant helps to prevent aggregation of particles. These networks held apart the particles from each other and hence preventing physical contact between them which had successfully prevented aggregation. At 40ºC however, the high temperature had caused alteration of trehalose as the cryoprotectant. This caused reduction of the glassy network efficiency and hence leading to the aggregation of nanoparticles. The effect of aging on the average particles size and polydispersity index of chitosan-coated rifampicin-loaded nanoparticles was also evaluated at the three different temperatures.

The average nanoparticles size was shown to be increased overtime; however the extent of increment between the temperatures differs (Table 6). At 4ºC, the increment was slight and slow as compared to the other two temperatures. At 25ºC and 40ºC, the agglomeration of the particles could be clearly seen and the increment in the particles size over time was more pronounced.

The redispersibility of the nanoparticles kept at 4ºC was fast, whilst for particles kept at 25ºC and 40ºC, the reconstitution of dried nanoparticles was difficult and needed the usage of vortex mixer. Based on this finding, the chitosan-coated nanoparticles should hence be stored at 4ºC to prevent the elimination of its physical nano-property.

***In vitro* drug release study and kinetics of release**

The *in vitro* release study was conducted in three different buffers to evaluate the effect of different pH on rifampicin release. The pH values chosen were corresponding to different segments of the gastrointestinal tract; pH 4.5 is the pH in the duodenum, pH 6.8 represents the jejunum and ileum, whilst pH 7.4 is the pH of the colon, as well as pH of the blood. Figure 5 showed the release profile of rifampicin from P (3HB-*co*-4HB) nanoparticles. There were presences of burst release in the first hour followed by a constant release until the 10th hour, during which 99.64%, 99.59% and 100% rifampicin was released at pH 4.5, 6.8 and 7.4 respectively. The results obtained illustrated that there were no significant different of rifampicin release between the three pH values.

This is in concordance with those obtained by other researchers who showed that the *in vitro* release of rifampicin from uncoated microspheres were not affected by medium pH [15]. The burst release could be attributed to the release of adsorbed rifampicin on the nanoparticles' surface. The encapsulated rifampicin which was blended with the copolymer matrix is released at a much slower rate, theoretically via diffusion through pores formed during the solvent evaporation process. In order to determine the drug release mechanism of rifampicin from the nanoparticles, the release kinetics were studied by fitting the *in vitro* data in various mathematical models; zero-order kinetics, first-order kinetics, Hixson-Crowell release model, Higuchi release model and Korsmeyer-Peppas release model

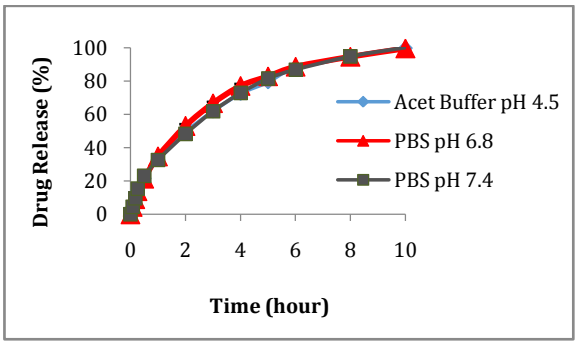

Fig. 5: *In vitro* drug release profiles in acetate buffer pH 4.5, phosphate-buffered saline pH 6.8 and phosphate-buffered saline pH 7.4

(PBS : Phosphate-buffered saline, Acet Buffer : Acetate buffer)

Table 7 shows the R^2 values of the different models use in the evaluation of the release kinetics at the three pH values. The R^2 values of first-order kinetics were higher than zero-order kinetics, showing that the release of drug from the nanoparticles is dependent on its concentration. The Higuchi's equation also showed high linearity, indicating that the release is via diffusion; whilst the high linearity in the Hixson-Crowell models describes that the drug is releases via dissolution and changes in the particles diameter and surface area. The result of Higuchi's and Hixson-Crowell were further confirmed by the Korsmeyer-Peppas models, in which the *n* value obtained, which were around 0.5 and 0.6 showed that the release of drug was via non-fickian or anomalous diffusion. This means that the release mechanism was a combination of both diffusion and erosion controlled [10,16]. The release study conducted on chitosan-coated rifampicin-loaded nanoparticles showed a slightly different profile as in Figure 6. At pH 4.5, 81.30% of encapsulated rifampicin was released in 10 hours.

This is because at pH 4.5, the chitosan layers absorb water and expand which caused the formation of viscous layer around the nanoparticles and hence retarding the drug release. As opposed to pH 7.4 and 6.8, 88.96% and 99.50% respectively were released in the same length of time. The *in vitro* release data were also fitted into different kinetic models, and the results were presented in Table 8. The release data of rifampicin from the chitosan-coated nanoparticles were best fitted in the first order kinetic, as compared to zero order at all pH values and this means that the release is concentration dependent. The release data were also found to fit well with Hixson-Crowell model, which implicates that the drug release is suggested to be via dissolution of the nanoparticles surface.

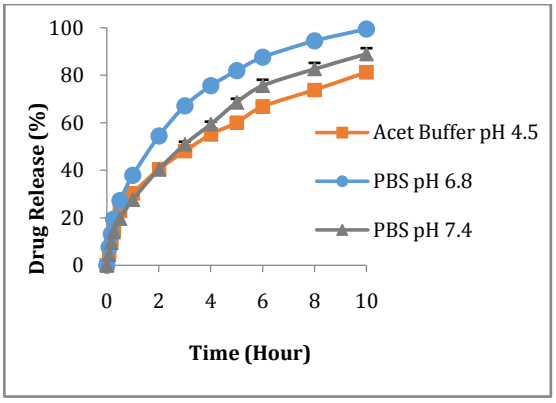

Fig. 6: *In vitro* drug release profiles of chitosan-coated rifampicin-loaded nanoparticles in acetate buffer pH 4.5, phosphate-buffered saline pH 6.8 and phosphate-buffered saline pH 7.4.

(PBS : Phosphate-buffered saline, Acet Buffer : Acetate Buffer)

The Higuchi model was also used and the R^2 value obtained fitted well with all three pH values, showing that the drug release was also via diffusion. The result obtained from the Korsmeyer-Peppas model on the other hand explained that the combination of both methods; diffusion and dissolution are the possible method of drug release from the chitosan-coated nanoparticles. The mechanism of rifampicin release from chitosan-coated nanoparticles at pH 4.5 was found to be through fickian's diffusion, as apparent by the *n* value obtained from Korsmeyer-Peppas kinetic model. The *n* value was 0.42. Chitosan layer on the nanoparticles surface retarded the diffusion of the encapsulated drug molecules because they have to work their way out through the highly swollen and entangled chitosan network before they could reach the external environment. In addition, the coating layer of chitosan prevented the exposure of nanoparticles surface to the environmental buffer and minimizes the surface dissolution. Due to this factor, diffusion was more prominent as compared to surface dissolution at pH 4.5. The network of chitosan on the nanoparticles surface when subjected to pH 6.8 and 7.4 may not swell as much. This led to the *n* value of more than 0.45 for both pH values, which means that the released of drugs were via non-fickian or anomalous diffusion. Nevertheless, a general comparison between Hixson-Crowell and Higuchi's model would suggest that the release is more prominently via diffusion. In addition, the fact that the polyhydroxybutyrate-type of polymer has slow dissolution rate also plays a major role in determining that diffusion would definitely be the main mechanism of release [3].

CONCLUSION

In conclusion, the novel P (3HB-*co*-4HB) copolymer from *Cupriavidus sp.* USMAA1020 has a huge potential to be developed as nanoparticles for controlled drug delivery system. The possibility of various kinds of modifications that could be done on the nanoparticles promises productions of nanoparticles with excellent properties which could be tailored to different applications. More creative and innovative research and development works shall be carried out to fully discover the potential of this copolymer. The association of nanoparticles from P (3HB-*co*-4HB) copolymer with rifampicin in this study might also serve as an excellent breakthrough for a better treatment outcome for tuberculosis patients in the future.

ACKNOWLEDGMENT

We would like to express our gratitude to Ministry of Science, Technology and Innovation Malaysia for providing financial support in ensuring the completion and success of this study.

ABBREVIATIONS

ANOVA, Analysis of Variance; DCM, Dichloromethane; DLS, Dynamic Light Scattering; EE, Encapsulation Efficiency; FTIR, Fourier-Transformed Infra-Red; KBr, Potassium Bromide; MWCO, Molecular Weight Cut-off; PDI, Polydispersity Index; TB, Tuberculosis; PHB, Polyhydroxybutyrate; PVA, Polyvinyl alcohol; P (3HB-*co*-4HB), Poly (3-hydroxybutyrate-*co*-4-hydroxybutyrate); RIF, Rifampicin; RPM, Revolution Per Minute; TEM, Transmission Electron Microscopy; UV/VIS, Ultraviolet/Visible.

REFERENCES

1. Powell J.J., Faria N., Thomas-McKay E., Pele L.C. Origin and fate of dietary nanoparticles and microparticles in the gastrointestinal tract. Journal of Autoimmunity. 2010.34(3):J226-J33.
2. Amirul A.A., Yahya A.R.M., Sudesh K., Azizan M.N.M., Majid M.I.A. Biosynthesis of poly(3-hydroxybutyrate-co-4-hydroxybutyrate) copolymer by Cupriavidus sp. USMAA1020 isolated from Lake Kulim, Malaysia. Bioresource Technology. 2008.99(11):4903-9.
3. Pouton C.W., Akhtar S. Biosynthetic polyhydroxyalkanoates and their potential in drug delivery. Advanced Drug Delivery Reviews. 1996.18(2):133-62.
4. Errico C., Bartoli C., Chiellini F., Chiellini E. Poly(hydroxyalkanoates)-Based Polymeric Nanoparticles for Drug Delivery. Journal of Biomedicine and Biotechnology. 2009.
5. Shishatskaya E., Voinova O., Goreva A., Mogilnaya O., Volova T. Biocompatibility of polyhydroxybutyrate microspheres: in vitro and in vivo evaluation. Journal of Materials Science: Materials in Medicine. 2008.19(6):2493-502.
6. Maia J.L., Santana M.H.A., Re M.I. The effect of some processing conditions on the characteristics of biodegradable microspheres obtained by an emulsion solvent evaporation process. Brazilian Journal of Chemical Engineering. 2004.21(1):1-12.
7. Salman M.A., Sahin A., Onur M.A., Oge K., Kassab A., Aypar U. Tramadol encapsulated into polyhydroxybutyrate microsphers: *in vitro* release and epidural analgesic effect in rats. Acta Anaesthesiol Scand. 2003.47:1006-12.
8. Tripathi A., Gupta R., Saraf S.A. PLGA Nanoparticles of Anti Tubercular Drug: Drug Loading and Release Studies of a Water In-Soluble Drug. International Journal of PharmTech Research. 2010.2(3):2116-23.
9. Patel H.V., Patel B.G., Patel V.A. Preparation and Physicochemical Characterization of Methotrexate PLGA Microparticles. International Journal of Pharmaceutical Research. 2010.2(1):75-81.
10. Date P.V., Samad A., Devarajan P.V. Freeze Thaw: A Simple Approach for Prediction of Optimal Cryoprotectant for Freeze Drying. AAPS PharmSciTech. 2010.11(1):304-13.
11. Wei Y.H., Chen W.C., Huang C.K., Wu H.S., Sun Y.M., Lo C.W., Janarthanan O.M. Screening and Evaluation of Polyhydroxybutyrate-Producing Strains from Indigenous Isolate Cupriavidus taiwanensis Strains. Int J Mol Sci.12(1):252-65.
12. Aarthi N., Ramana K.V. Identification and Characterization of Polyhydroxybutyrate producing Bacillus cereus and Bacillus mycoides strains. International Journal of Environmental Sciences. 2011.1(5).
13. Bayari S., Severcan F. FTIR study of biodegradable biopolymers : P(3HB), P(3HB-*co*-4HB) and P(3HB-*co*-3HV). Journal of Molecular Structure. 2005.744-747:529-34.
14. Granja P.L., Silva A.I.N., Borges J.P., Barrias C.C., Amaral I.F. Preparation and Characterization of Injectable Chitosan-Hydroxyapatite Microspheres. Key Engineering Materials. 2004.254-256:573-6.
15. Manca M.L. Chitosan and PLGA Microspheres as Drug Delivery System Against Pulmonary Mycobacteria Infections: University of Cagliari, 2009.
16. Dash V., Mishra S.K., Singh M., Goyal A.K., Rath G. Release Kinetic Studies of Aspirin Microcapsules from Ethyl Cellulose, Cellulose Acetate Phthalate and their Mixtures by Emulsion Solvent Evaporation Method. Scientia Pharmaceutica. 2010.78:93-101.